Supporting Information For

Quantifying the Effects of Quadrupolar Sink via ^{15}N Relaxation Dynamics in Metronidazoles Hyperpolarized via SABRE-SHEATH

Jonathan R. Birchall,[a] Mohammad S. H. Kabir,[a] Oleg G. Salnikov,[b,c,d] Nikita V. Chukanov,[b,c] Alexandra Svyatova,[b,c] Kirill V. Kovtunov,[b,c] Igor V. Koptyug,[b,c] Juri G. Gelovani,[a,e] Boyd M. Goodson,[f] Wellington Pham,[g,h] and Eduard Y. Chekmenev[a,i]*

[a] Department of Chemistry, Integrative Biosciences (Ibio), Wayne State University, Karmanos Cancer Institute (KCI), Detroit, Michigan 48202, United States

[b] International Tomography Center, SB RAS, 3A Institutskaya St., Novosibirsk 630090, Russia

[c] Novosibirsk State University, 2 Pirogova St., Novosibirsk 630090, Russia

[d] Boreskov Institute of Catalysis SB RAS, 5 Acad. Lavrentiev Pr., Novosibirsk 630090, Russia

[e] United Arab Emirates University, Al Ain, United Arab Emirates

[f] Department of Chemistry and Biochemistry and Materials Technology Center, Southern Illinois University, Carbondale, Illinois 62901, United States

[g] Vanderbilt University Institute of Imaging Science (VUIIS), Department of Radiology, Vanderbilt University Medical Center (VUMC), Department of Biomedical Engineering, Vanderbilt University, Vanderbilt-Ingram Cancer Center (VICC), Nashville, Tennessee 37232-2310, United States

[h] Russian Academy of Sciences, Leninskiy Prospekt 14, Moscow, 119991, Russia

Table of Contents

1. ^{15}N SABRE-SHEATH hyperpolarization

The sample solutions for SABRE hyperpolarization were prepared with different ratios (0.5:20, 1:20 and 2:20) of [catalyst]:[substrate], where different concentrations (0.5 mM, 1 mM, and 2 mM) of IrIMes catalyst were added to different Eppendorf tubes containing 0.6 mL of methanol-d_4 solvent and 20 mM of one of the two studied ^{15}N-labelled metronidazole isotopologues (MNZ-$^{15}N_2$ and MNZ-$^{15}N_3$). A measured mass of ^{15}N-labelled metronidazole isotopologue *e.g.*, MNZ-$^{15}N_2$ or MNZ-$^{15}N_3$, was transferred to a plastic Eppendorf tube and mixed with methanol-d_4 to create a concentration of 40 mM. Then, 0.3 ml methanol-d_4 with metronidazole isotopologue, and 0.3ml of methanol-d_4 with IrIMes catalyst was added to yield a 1:20 mM ratio of [IrIMes catalyst]:[isotopologue of ^{15}N-labelled metronidazole], which was then transferred to a medium-wall 5 mm NMR tube. By the same procedure, a ratio of 0.5:20 mM and 2:20 mM of [catalyst]:[substrate] was also prepared. The freshly prepared solution was then flushed with ultra-pure argon gas for 2 min. All prepared samples were used for SABRE activation immediately after argon gas was bubbled, and all data from SABRE-SHEATH hyperpolarization experiments were collected within five hours of primary sample preparation.

The IrIMes catalyst precursor[1] for the SABRE study was synthesized by following our previously published study[2]. To achieve optimal catalyst activation[3], the prepared NMR tubes were placed in the magnetic field and bubbled with pH_2 at a flow rate of 40 sccm for 100 min.

For all the experiments, the NMR tube containing 0.6 mL aliquot of sample was placed in the center of the mu-metal shield and connected to the SABRE hyperpolarization setup, which was followed from the previous study.[4] During and after the catalyst activation, all NMR spectra were recorded using a 1.4 T Benchtop NMR spectrometer (NMR Pro 60, Nanalysis, Canada) using varying flow rate at a range of 10 to 120 standard cubic centimeters per minute (sccm). The flow rate was controlled by a mass flow controller, with 96 psig overpressure of pH_2 gas in the NMR tube at room temperature (~22-23 °C). The reference spectrum of neat pyridine-^{15}N, which was thermally polarized, was collected using ^{15}N spectroscopy without proton decoupling in the same manner as for all ^{15}N spectra from HP of different ^{15}N-labelled metronidazole isotopologues (MNZ-$^{15}N_2$ and MNZ-$^{15}N_3$) with the exception for the number of scans (8) and the polarization recovery time (600 s) between these scans.

The temperature dependence study was performed with a range of 0 °C to 50 °C, where different temperatures were achieved by placing the NMR tube containing substrate and catalyst solution in either an ice- or hot water bath before the spectra collection procedure with the same SABRE setup.

2. Calculation of ^{15}N signal enhancements (ε_{15N}) and ^{15}N polarization (P_{15N}) values

The signal enhancement values for the 1.4 T benchtop NMR spectrometer were calculated by using the following equation from Shchepin et al [5]:

$$\varepsilon_{15N} = \frac{S_{HP}}{S_{REF}} \times \frac{C_{REF}}{C_{HP}} \times \frac{A_{REF}}{A_{HP}} \times \frac{N_{REF}}{N_{HP}}$$

where S_{HP} and S_{REF} are the NMR signal intensities for HP different ^{15}N-labelled metronidazole isotopologues (MNZ-$^{15}N_2$ and MNZ-$^{15}N_3$) and the thermally polarized signal reference (neat pyridine-^{15}N) samples correspondingly, C_{REF} and C_{HP} are the effective isotope concentrations of the thermally polarized signal reference (12.4 M for neat pyridine-^{15}N) and of different ^{15}N-labelled metronidazole isotopologues (MNZ-$^{15}N_2$ and MNZ-$^{15}N_3$), respectively. Here, the acquired spectra were collected using a single scan, 90-degree tipping angle, 10dB receiver gain, 400 ppm spectral width, and 4096 acquisition points. The concentration of MNZ-$^{15}N_2$ and MNZ-$^{15}N_3$ was adjusted for the evaporation fraction as mentioned in our previous paper[6], and for the catalyst-binding (for different concentration of catalyst, 20 mM of MNZ-$^{15}N_2$ or MNZ-$^{15}N_3$ remains in the catalyst bound state and no changes of the peak intensities observed), because all HP resonances observed in Figure 1c and 1d originate from the free MNZ-$^{15}N_3$ pool. For example, for a 40 mM evaporation-adjusted concentration, 40 mM was multiplied by (17/20), where 20 corresponds to the initial 20 mM MNZ-$^{15}N_2$ or MNZ-$^{15}N_3$ concentration, and 17 is the 17-mM concentration of the free MNZ-$^{15}N_2$ or MNZ-$^{15}N_3$ substrate after binding of 3 equivalents to the catalyst for its 1 mM concentration: one equivalent in an axial position of the complex and two equivalents in the equatorial positions. The same criteria were applied for both 0.5 mM and 2 mM concentrations of Ir-IMes catalyst,

where the substrate concentration would be 18.5 mM and 14 mM respectively. A_{REF} and A_{HP} are the solution cross-sections in the NMR tube of the thermally polarized signal reference and HP samples respectively (A_{REF}/A_{HP} was ~1.85 as described previously[7]). N_{REF} and N_{HP} are the numbers of symmetrical sites per molecule (1 for both cases) for the thermally polarized signal reference and HP samples respectively. The percentage of polarized ^{15}N spins (P_{15N}) was calculated by multiplying signal enhancement ε_{15N} by the equilibrium ^{15}N spin polarization ($\%P_{15N}$) at 1.4 T and 298 K: $4.9\times10^{-5}\%$.

The collected spectra of all ^{15}N-labelled metronidazole isotopologue samples and the neat pyridine-^{15}N reference (showed in Figure 1e) were acquired using one scan and 8 scans respectively. The pre-acquisition delay on the thermal reference scan was 600 seconds to ensure a reliable equilibrium thermal polarization of ^{15}N spins was achieved in the signal reference.

2.1 $^{15}N_1$ site in metronidazole-$^{15}N_2$

The integral signal value of MNZ-$^{15}N_2$ (S_{HP}) in $^{15}N_1$ site is 2.123 in Figure 1f and the thermally polarized signal reference (S_{REF}) is 0.0359. As previously mentioned, C_{REF} for neat pyridine-^{15}N is 12.4 M and C_{HP} is 0.014 M. A_{REF}/A_{HP} is 1.85 and N_{REF}/N_{HP} is 1.

By using the above-mentioned values in the ^{15}N signal enhancements (ε_{15N}) and $\%P_{15N}$ are:

$$\varepsilon_{15N1} = \frac{2.123}{0.0359} \times \frac{12.4}{0.014} \times 1.85 \times 1 = 9.8 * 10^4 \qquad \%P_{15N1} = 9.8*10^4*4.9*10^{-5}=4.8\%$$

2.2 $^{15}N_3$ site of metronidazole-$^{15}N_2$

The integral signal value of MNZ-$^{15}N_2$ (S_{HP}) in $^{15}N_1$ site is 1.885 in Figure 1f and all other values are same. So, the ^{15}N signal enhancements (ε_{15N}) and $\%P_{15N}$ are:

$$\varepsilon_{15N1} = \frac{1.885}{0.0359} \times \frac{12.4}{0.014} \times 1.85 \times 1 = 8.7 * 10^4 \qquad \%P_{15N3} = 8.7*10^4*4.9*10^{-5}=4.3\%$$

2.3 $^{15}N_1$ site of metronidazole-$^{15}N_3$

The integral signal value of MNZ-$^{15}N_3$ (S_{HP}) in $^{15}N_1$ site is 6.842 in Figure 1g and all other values are same. So, the ^{15}N signal enhancements (ε_{15N}) and $\%P_{15N}$ are:

$$\varepsilon_{15N1} = \frac{6.842}{0.0359} \times \frac{12.4}{0.014} \times 1.85 \times 1 = 3.2 * 10^5 \qquad \%P_{15N1} = 3.2*10^5*4.9*10^{-5}=15.4\%$$

2.4 $^{15}N_3$ site of metronidazole-$^{15}N_3$

The integral signal value of MNZ-$^{15}N_3$ (S_{HP}) in $^{15}N_1$ site is 5.192 in Figure 1g and all other values are same. So, the ^{15}N signal enhancements (ε_{15N}) and $\%P_{15N}$ are:

$$\varepsilon_{15N1} = \frac{5.192}{0.0359} \times \frac{12.4}{0.014} \times 1.85 \times 1 = 2.4 * 10^5 \qquad \%P_{15N3} = 2.4*10^5*4.9*10^{-5}=11.7\%$$

2.5 $^{15}NO_2$ site of metronidazole-$^{15}N_3$

The integral signal value of MNZ-$^{15}N_3$ (S_{HP}) in $^{15}N_1$ site is 7.78 in Figure 1g and all other values are same. So, the ^{15}N signal enhancements (ε_{15NO2}) and $\%P_{15N}$ are:

$$\varepsilon_{15NO2} = \frac{7.78}{0.0359} \times \frac{12.4}{0.014} \times 1.85 \times 1 = 3.6 * 10^5 \qquad \%P_{15NO2} = 3.6*10^5*4.9*10^{-5}=17.5\%$$

3. Figures S1-S3

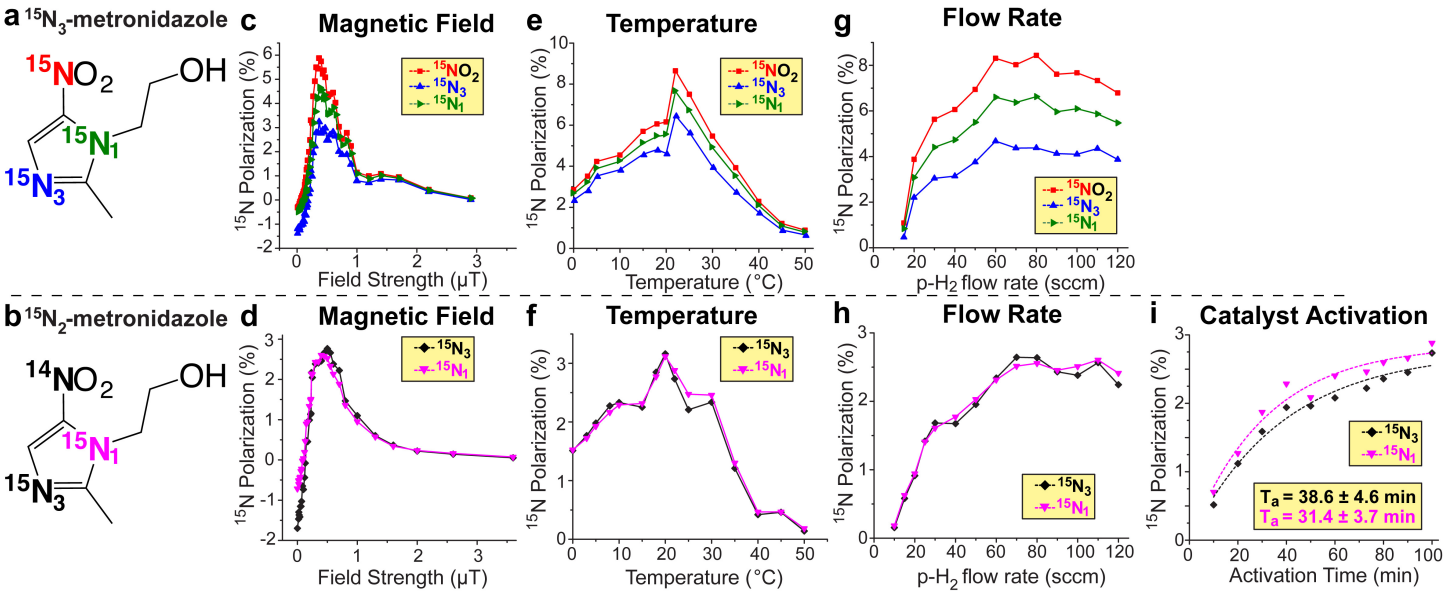

Figure S1. a) chemical structure of metronidazole-$^{15}N_3$; b) chemical structure of metronidazole-$^{15}N_2$; c) magnetic field dependence of the spin-relayed SABRE-SHEATH polarization transfer process for metronidazole-$^{15}N_3$ (experiment performed at room temperature, 70 sccm flow rate, 94 psig p-H_2 overpressure); d) magnetic field dependence of the spin-relayed SABRE-SHEATH polarization transfer process for metronidazole-$^{15}N_2$ (experiment performed at room temperature, 70 sccm flow rate, 94 psig p-H_2 overpressure); e) magnetic field dependence of the spin-relayed SABRE-SHEATH polarization transfer process for metronidazole-$^{15}N_3$ (experiment performed at ~0.4 μT, 70 sccm flow rate, 94 psig p-H_2 overpressure); f) magnetic field dependence of spin-relayed SABRE-SHEATH polarization transfer process for metronidazole-$^{15}N_2$ (experiment performed at ~0.4 μT, 70 sccm flow rate, 94 psig p-H_2 overpressure); g) p-H_2 flow rate dependence of the spin-relayed SABRE-SHEATH polarization transfer process for metronidazole-$^{15}N_3$ (experiment performed at ~0.4 μT, room temperature, 94 psig p-H_2 overpressure); h) p-H_2 flow rate dependence of the spin-relayed SABRE-SHEATH polarization transfer process for metronidazole-$^{15}N_2$ (experiment performed at ~0.4 μT, room temperature, 94 g p-H_2 overpressure); i) Ir-IMes catalyst activation curve of the spin-relayed SABRE-SHEATH polarization transfer process for metronidazole-$^{15}N_2$ (experiment performed at ~0.4 μT, room temperature, 94 psig p-H_2 overpressure, 70 sccm p-H_2 flow rate). Note: for all graphs, the solid connecting lines are added to guide the eye, whereas the dotted curves are exponential fits to the data for the build-up process.

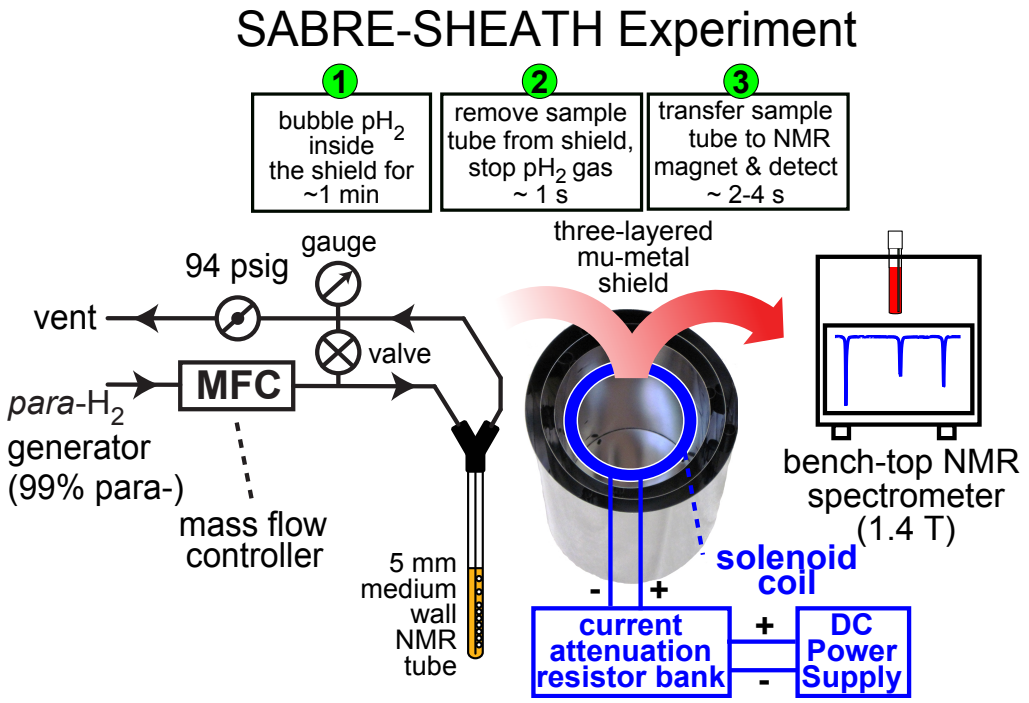

Figure S2. The diagram of experimental setup.

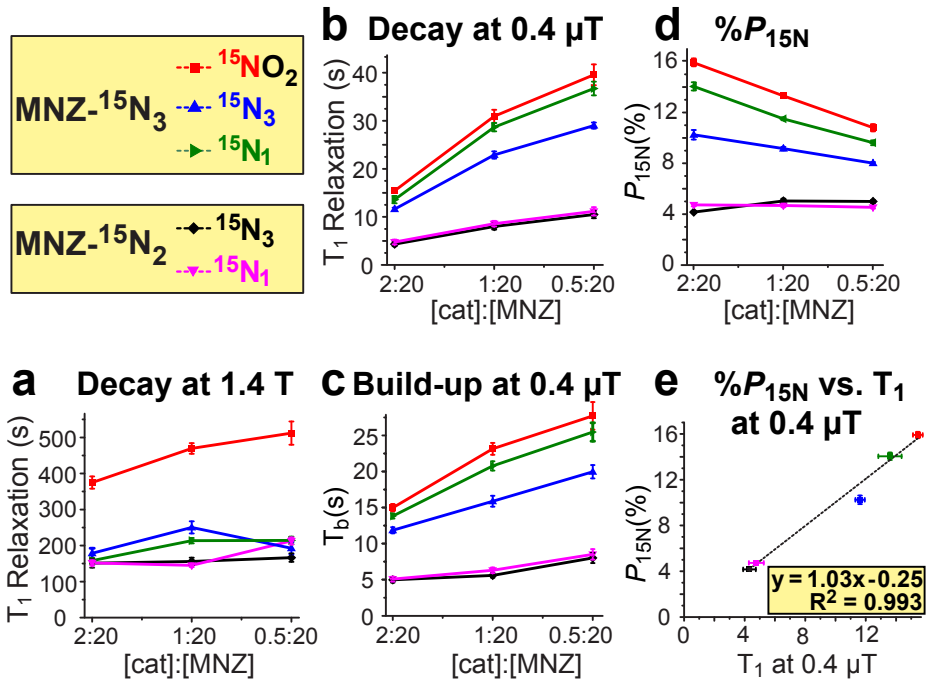

Figure S3. a) Dependence of ^{15}N polarization T_1 decay at 1.4 T on the catalyst-to-substrate concentration ratio. b) Same as (a), but at 0.4 μT. c) Dependence of ^{15}N polarization build-up time constant (T_b) at 0.4 μT on the catalyst-to-substrate concentration ratio. d) Dependence of ^{15}N steady-state polarization value (achieved after 1 min. of build-up) on the catalyst-to-substrate concentration ratio. e) Dependence of $\%P_{15N}$ on ^{15}N T_1 at 0.4 μT, using 2 mM IrIMes catalyst concentration and 20 mM MNZ-$^{15}N_3$ or MNZ-$^{15}N_2$. The solid connecting lines are added to guide the eye; the dotted line in (e) is a linear fit to the data. All experiments are performed in CD_3OD.

4. Table S1. Summary of relaxation dynamics results.

[Catalyst]:[isotopologue]			^{15}N T_b at 0.4 µT (sec)	^{15}N T_1 at 0.4 µT (sec)	^{15}N T_1 at 1.4T (sec)	^{15}N T_1 at the Earth's field (sec)	^{15}N $\%P_{max}$ (%) from fitting	Highest $\%P_{15N}$ Recorded
1:20	**MNZ-$^{15}N_3$**	**NO_2**	23.1 ± 0.8	30.9 ± 1.4	470 ± 15	133 ± 14	13.3 ± 0.2	13.5 ± 0.7
		N_3	15.9 ± 0.8	22.9 ± 0.8	250 ± 17	169 ± 13	9.2 ± 0.1	9.0 ± 0.5
		N_1	20.8 ± 0.7	28.7 ± 0.9	214 ± 7	144 ± 12	11.5 ± 0.1	11.4 ± 0.6
	MNZ-$^{15}N_2$	**N_3**	5.6 ± 0.3	8.0 ± 0.6	156 ± 11	43 ± 4	5.1 ± 0.2	5.9 ± 0.3
		N_1	6.3 ± 0.4	8.6 ± 0.6	145 ± 5	48 ± 4	4.7 ± 0.1	5.3 ± 0.3
2:20	**MNZ-$^{15}N_3$**	**NO_2**	15.0 ± 0.5	15.4 ± 0.3	375 ± 17	92 ± 4	15.9 ± 0.3	17.5 ± 0.9
		N_3	11.8 ± 0.4	11.6 ± 0.3	179 ± 14	100 ± 17	10.3 ± 0.4	11.7 ± 0.6
		N_1	13.8 ± 0.4	13.6 ± 0.8	158 ± 8	95 ± 4	14.1 ± 0.3	15.4 ± 0.8
	MNZ-$^{15}N_2$	**N_3**	5.0 ± 0.4	4.3 ± 0.4	151 ± 12	30 ± 1	4.2 ± 0.1	4.3 ± 0.2
		N_1	5.1 ± 0.4	4.8 ± 0.5	152 ± 7	31 ± 1	4.7 ± 0.1	4.8 ± 0.2
0.5:20	**MNZ-$^{15}N_3$**	**NO_2**	27.7 ± 1.9	39.6 ± 2.2	512 ± 32	103 ± 11	10.8 ± 0.3	10.1 ± 0.5
		N_3	20.0 ± 0.9	29.0 ± 0.6	193 ± 17	118 ± 9	8.0 ± 0.1	7.8 ± 0.4
		N_1	25.5 ± 1.3	36.7 ± 1.4	214 ± 10	111 ± 10	9.6 ± 0.2	9.1 ± 0.5
	MNZ-$^{15}N_2$	**N_3**	8.0 ± 0.7	10.5 ± 0.8	166 ± 12	47 ± 2	5.0 ± 0.1	4.9 ± 0.3
		N_1	8.5 ± 0.7	11.2 ± 0.9	213 ± 10	50 ± 3	4.5 ± 0.1	4.4 ± 0.2

5. ^{15}N True FIST MRI of HP metronidazole-$^{15}N_2$ and HP metronidazole-$^{15}N_3$

Before the experiments all samples were activated by bubbling p-H_2 through the solution for 1 hour, the flow rate was 8 sccm and 24 psig.

^{15}N-TrueFISP MRI XY (axial) projection. At the beginning, p-H_2 was bubbled through the solution in the NMR tube placed into mu-metal magnetic shield with a flow rate of 70 sccm for 1 minute. The NMR tube was also pressurized at 24 psig. After that, the p-H_2 flow was stopped and then NMR tube was moved to the Bruker NMR spectrometer (9.4 T), transfer time was approximately 20 seconds. 2D images were acquired using TrueFISP pulse sequence with repetition time (TR) = 62.5 ms and echo time (TE) = 3.6 ms. Receiver gain (RG) was 2050. Acquisition spectral width (SW) was 5.0 kHz, spatial resolution was 0.975×0.975 mm^2/pixel. Field of view was 3.1×3.1 cm^2. Acquisition matrix was 32×32, it was zero-filled to matrix size of 512×512 (Figures 4a and 4b). The flip angle was 15^o. Total acquisition time of a single average was 2.0 seconds.

^{15}N-TrueFISP MRI XZ (coronal) projection. At the beginning, p-H_2 was bubbled through the solution in the NMR tube placed into mu-metal magnetic shield with a flow rate of 70 sccm for 1 minute. The NMR tube was also pressurized at 24 psig. After that, the p-H_2 flow was stopped and then NMR tube was moved to the Bruker NMR spectrometer (9.4 T), transfer time was approximately 20 seconds. 2D images were acquired using TrueFISP pulse sequence with repetition time (TR) = 62.5 ms and echo time (TE) = 2 ms. Receiver gain (RG) was 2050. Acquisition spectral width (SW) was 10 kHz, spatial resolution was 0.894×0.894 mm^2/pixel. Field of view was 2.9×2.9 cm^2. Acquisition matrix was 32×32, it was zero-filled to matrix size of 512×512 (Figures 4c and 4d). The flip angle was 15^o. Eight averages were acquired during 16.7 seconds.

The signal-to-noise ratio of the maximum intensity pixel (SNR_{MAX}) was computed as follows:

$$SNR_{MAX} = \frac{max\ intensity\ (Area\ of\ the\ signal) - mean\ intensity(Area\ of\ the\ noise)}{std\ (Area\ of\ the\ noise)}$$

The area of the noise was selected as one of the top corners (8x8 pixels). All image processing and computation was performed using MATLAB.

6. Statement of Authors' Contributions

J.R.B. performed initial hyperpolarization experiments and analyzed the results. M.S.H.K. final data acquisition, performed data processing, data analysis and prepared some figures. N.V.C. synthesized ^{15}N-labeled isotopologues and performed their purification. A.S. performed ^{15}N MRI visualization of ^{15}N-hyperpolarized ^{15}N-labeled isotopologues. O.G.S., N.V.C., K.V.K., I.V.K., B.M.G., M.S.H.K. and E.Y.C. discussed the results and proof-read the manuscript which was written by E.Y.C. and J.R.B. J.G.G. discussed with E.Y.C. the biomedical aspects of metronidazole use in biomedicine for preparation of the manuscript and proof-read the manuscript.

6. References Used in Supporting Information

1. M. J. Cowley, R. W. Adams, K. D. Atkinson, M. C. Cockett, S. B. Duckett, G. G. Green, J. A. Lohman, R. Kerssebaum, D. Kilgour and R. E. Mewis, *Journal of the American Chemical Society*, 2011, **133**, 6134-6137.
2. D. A. Barskiy, K. V. Kovtunov, I. V. Koptyug, P. He, K. A. Groome, Q. A. Best, F. Shi, B. M. Goodson, R. V. Shchepin and A. M. Coffey, *Journal of the American Chemical Society*, 2014, **136**, 3322-3325.
3. M. L. Truong, F. Shi, P. He, B. Yuan, K. N. Plunkett, A. M. Coffey, R. V. Shchepin, D. A. Barskiy, K. V. Kovtunov and I. V. Koptyug, *The Journal of Physical Chemistry B*, 2014, **118**, 13882-13889.
4. T. Theis, M. L. Truong, A. M. Coffey, R. V. Shchepin, K. W. Waddell, F. Shi, B. M. Goodson, W. S. Warren and E. Y. Chekmenev, *Journal of the American Chemical Society*, 2015, **137**, 1404-1407.
5. R. V. Shchepin, L. Jaigirdar, T. Theis, W. S. Warren, B. M. Goodson and E. Y. Chekmenev, *The Journal of Physical Chemistry C*, 2017, **121**, 28425-28434.
6. R. V. Shchepin, J. R. Birchall, N. V. Chukanov, K. V. Kovtunov, I. V. Koptyug, T. Theis, W. S. Warren, J. G. Gelovani, B. M. Goodson and S. Shokouhi, *Chemistry–A European Journal*, 2019, **25**, 8829-8836.
7. M. L. Truong, T. Theis, A. M. Coffey, R. V. Shchepin, K. W. Waddell, F. Shi, B. M. Goodson, W. S. Warren and E. Y. Chekmenev, *J. Phys. Chem. C*, 2015, **119**, 8786–8797.